Ocean Dynamics (2005) 55: 326–337
DOI 10.1007/s10236-005-0001-x

Hans Burchard · Eric Deleersnijder · Andreas Meister

Application of modified Patankar schemes to stiff biogeochemical models for the water column

Received: 29 September 2004 / Accepted: 14 January 2005 / Published online: 8 November 2005

Abstract In this paper, we apply recently developed positivity preserving and conservative Modified Patankar-type solvers for ordinary differential equations to a simple stiff biogeochemical model for the water column. The performance of this scheme is compared to schemes which are not unconditionally positivity preserving (the first-order Euler and the second- and fourth-order Runge–Kutta schemes) and to schemes which are not conservative (the first- and second-order Patankar schemes). The biogeochemical model chosen as a test ground is a standard nutrient–phytoplankton–zooplankton–detritus (NPZD) model, which has been made stiff by substantially decreasing the half saturation concentration for nutrients. For evaluating the stiffness of the biogeochemical model, so-called numerical time scales are defined which are obtained empirically by applying high-resolution numerical schemes. For all ODE solvers under investigation, the temporal error is analysed for a simple exponential decay law. The performance of all schemes is compared to a high-resolution high-order reference solution. As a result, the second-order modified Patankar–Runge–Kutta scheme gives a good agreement with the reference solution even for time steps 10 times longer than the shortest numerical time scale of the problem. Other schemes do either compute negative values for non-negative state variables (fully explicit schemes), violate conservation (the Patankar schemes) or show low accuracy (all first-order schemes).

Responsible Editor: Phil Dyke

H. Burchard (✉)
Baltic Sea Research Institute Warnemünde, Seestraße 15, 18119 Rostock-Warnemünde, Germany
E-mail: hans.burchard@io-warnemuende.de

E. Deleersnijder
G. Lemaî tre Institute of Astronomy and Geophysics (ASTR) and Centre for Systems Engineering and Applied Mechanics (CESAME), Université catholique de Louvain,
4 Avenue G. Lemaî tre, 1348 Louvain-la-Neuve, Belgium
E-mail: ericd@astr.ucl.ac.be

A. Meister
Faculty of Mathematics and Informatics, University of Kassel,
Heinrich-Plett-Str. 40, 34109 Kassel, Germany
E-mail: meister@mathematik.uni-kassel.de

1 Introduction

Stiff problems are widely spread in almost all areas of science and technology. Examples are given by chemical reaction systems or laminar as well as turbulent viscous fluid flow. Several further occurrences of stiffness can be found in electronics, mechanics, meteorology, oceanography and biology. Water column chemistry, e.g. iron chemistry (see Weber et al. 2005), and diagenetic processes in the sediment (see e.g. Soetaert et al. 1996) often pose stiff problems in oceanography. For a collection of several stiff problems in atmospheric chemistry, see Sandu et al. (1997). For a detailed introduction to stiff problems we refer to the well-written textbooks by Hairer and Wanner (2004) and Hundsdorfer and Verwer (2003). Although, the expression stiffness is naturally used in an intuitive sense, there does not exist a comprehensive and general mathematical definition up to now. The reason for this fact is closely related to the extremely wide variety of origins of stiffness. In chemical reacting systems, stiffness is caused by vastly different rate coefficients which give rise to extremely different time scales in the solution of the system. A typical example is given by the so-called Robertson test case (Robertson 1966; Hairer and Wanner 2004), where the ratio of the largest to the smallest rate coefficient is 7.5×10^{8}. An additional indicator which is also often used for a classification of stiffness is related to the advantage of implicit versus explicit methods. Usually, a stable discretisation of stiff problems can only be attained by implicit time stepping techniques. The reason for this

fact often arises from the occurrence of large eigenvalues of the Jacobian of the underlying system of equations. The time-step size of an explicit scheme has to be chosen proportional to the reciprocal of the largest eigenvalue. Although implicit methods suffer from an additional computational effort due to the solution of a large, linear or non-linear system of equations arising in each time step, these schemes are usually to be preferred. Note that the matrix associated with the linear system is usually sparse, which is beneficial for iterative solution methods, see Meister (1998). It is worth mentioning, that besides the equation itself, the stiffness depends on the initial conditions. In this context an initial value problem is called stiff, if the solution possesses a large Lipschitz constant.

As mentioned above, the efficient discretisation of stiff problems is usually associated with implicit methods. However, implicit schemes suffer from the necessity of solving at least one linear or nonlinear system of equations per time step. In order to avoid this computational effort as long as the problem behaves non-stiff, one can employ combined explicit–implicit techniques whereby the transition is determined by means of a stiffness indicator based on either an error estimator or an estimator for the dominant eigenvalue of the Jacobian, see Hairer and Wanner (2004). For moderately stiff problems, different families of stabilised explicit Runge–Kutta methods are developed. Even though, for Runge–Kutta methods explicitly exclude A-stability, one can extend the stability domain in the direction of the negative axis. These methods are designed such that the stability function represents a Chebyshev polynomial. A representative of this type of schemes is the DUMKA method developed by Lebedev (2000) and Medovikov (1998). A very popular approach proposed by van der Houwen and Sommeijer (1980) is called RKC (Runge–Kutta–Chebyshev). An introduction to second-order RKC methods as well as second- and fourth-order ROCK methods (Orthogonal-Runge–Kutta–Chebyshev) recently designed by Abdulle (2001) and Abdulle and Medovikov (2001) can be found in Hundsdorfer and Verwer (2003). Stabilised Runge–Kutta methods are often efficient for the discretisation of semi-discrete equations arising within a method of lines approach applied to parabolic partial differential equations, see Verwer (1996) and van der Houwen (1996).

The collection of all A-stable methods represents a subset of the class of implicit schemes. For example the Θ-scheme belongs to this set if $\Theta \in [1/2, 1]$. Furthermore, implicit Runge–Kutta methods like the s-stage Lobatto IIIA/IIIB/IIIC of various even orders, the implicit midpoint rule as well as Radau IIA-scheme of order 3, 5, 7 are A-stable, whereas the A-stability of the SDIRK schemes depends on the choice of the incorporated parameter and several other implicit algorithms do not satisfy the requirement associated with A-stability, see Hairer et al. (2000), Hairer and Wanner (2004). Other efficient methods for stiff problems are linearly implicit Runge–Kutta methods also called Rosenbrock schemes as well as the A-stable BDF2 method which represents the most famous linear multi-step method of second order.

In a wide variety of applications, one is additionally faced with the fact that the quantities within the model are assumed to be nonnegative from a physical, biological or chemical point of view. Obviously, this property should also be guaranteed by the numerical method used. Algorithms satisfying this requirement are called positivity preserving methods. The enforcement of positivity usually yields a severe restriction on the step size. Upper bounds for the Θ-scheme can be found in Hundsdorfer and Verwer (2003). Furthermore, various conditions for positivity preservation of Runge–Kutta methods are presented by Horváth in a sequence of papers, see Horváth (1998) and the references therein. It is easily seen that the implicit Euler method is unconditionally positivity preserving. However, this method is only first-order accurate and thus often insufficient to resolve the phenomena of interest in an appropriate manner. On the other hand, the A-stable BDF2 method is second order but obviously anything but positivity-preserving due to the negative weight appearing within the formula. In order to achieve an unconditional positivity preserving scheme, one can modify the original forward Euler method or an explicit Runge–Kutta scheme by simply weighting the sink terms. This technique, also called source term linearisation, was originally proposed by Patankar (1980). Unfortunately, the application of this procedure for the discretisation of conservative systems usually yields a non-conservative scheme and thus often leads to an unrealistic growth of the involved quantities. A cure for the problem was recently suggested by Burchard et al. (2003) by introducing an additional modification of the production terms. These so-called Modified Patankar methods are conservative, unconditional positivity-preserving and first-order or second-order accurate depending on the underlying standard discretisation technique.

In this paper, we analyse the performance of these Patankar-type ODE solvers (Burchard et al. (2003)) for stiff water column problems and compare them to explicit schemes belonging to the Runge–Kutta hierarchy. After briefly introducing the general mathematical framework for coupled physical–biogeochemical models (Sect. Mathematical formulation) and describing the ODE solvers (Sect. Vertical discretisation and ODE solvers), the temporal accuracy of the ODE solvers investigated here is analysed in detail (Sect. Numerical time scales and temporal accuracy of ODE solvers). These models are then applied for the discretisation of a stiff model problem for the water column which has been obtained by modifying a parameter in a simple nutrient–phytoplankton–zooplankton–detritus (NPZD, see Sect. NPZD model) model for the Northern North Sea, see Sect. Model simulations. Finally, some conclusions are drawn (Sect. Conclusions).

2 Mathematical formulation

The general structure of a biogeochemical model with I state variables expressed as ensemble averaged concentrations is given by the following set of equations:

$$\partial_t c_i + \partial_z(w_i c_i - \nu'_t \partial_z c_i) = P_i(\underline{c}) - D_i(\underline{c}), \quad i = 1, \ldots, I \tag{1}$$

with $\underline{c} = (c_1, \ldots, c_I)^T$ denoting the concentrations of state variables. The vertical transport terms are included on the left-hand side of Eq. 1. There, w_i represents the vertical motion of the ecosystem component c_i (e.g. sinking or active swimming), and ν'_t represents the eddy diffusivity. The source and sink terms of the ecosystem component c_i are summarised in $P_i(\underline{c})$ and $D_i(\underline{c})$, respectively.

The right-hand side denotes the reaction terms, which are composed of contributions $d_{i,j}(\underline{c})$, which represent reactive fluxes from c_i to c_j, and in turn, $p_{i,j}(\underline{c})$ are reactive fluxes from c_j received by c_i:

$$P_i(\underline{c}) = \sum_{j=1}^{I} p_{i,j}(\underline{c}), \quad D_i(\underline{c}) = \sum_{j=1}^{I} d_{i,j}(\underline{c}), \tag{2}$$

with $d_{i,j}(\underline{c}) \geq 0$ and $p_{i,j}(\underline{c}) \geq 0$ for all i,j and $\underline{c}$. In the simple types of models considered here, the reactive terms do only exchange mass between state variables with

$$p_{i,j}(\underline{c}) = d_{j,i}(\underline{c}), \quad \text{for } i,j = 1, \ldots, I \tag{3}$$

and

$$p_{i,i}(\underline{c}) = d_{i,i}(\underline{c}) = 0, \quad \text{for } i = 1, \ldots, I. \tag{4}$$

In the case of vanishing transport terms (i.e. the vertical gradient terms on the left-hand side), one can easily conclude

$$\begin{aligned} d_t\left(\sum_{i=1}^{I} c_i\right) &= \sum_{i=1}^{I}(P_i(\underline{c}) - D_i(\underline{c})) \\ &= \sum_{i=1}^{I}\sum_{j=1}^{I}\left(p_{i,j}(\underline{c}) - d_{i,j}(\underline{c})\right) \\ &= \sum_{i=1}^{I}\left(p_{i,i}(\underline{c}) - d_{i,i}(\underline{c})\right) = 0 \end{aligned} \tag{5}$$

by using Eq. 3, which shows the conservation property of the governing equations.

For non-negative initial conditions $c_i(0) \geq 0$, one can easily show by a simple contradiction argument that the condition

$$d_{i,j}(\underline{c}) \longrightarrow 0 \quad \text{for } c_i \longrightarrow 0 \tag{6}$$

guarantees that for all state variables $c_i(t) \geq 0$ holds, i.e. they remain non-negative for all t.

3 Vertical discretisation and ODE solvers

Here, a splitting scheme will be applied to discretise the biogeochemical set of equations given by Eq. 1. In each time step of the two-time-level-scheme used here, first the transport part (advection and diffusion, see left-hand side) and then the reaction part (right-hand side) is solved numerically. For the diffusion part, the standard central-in-time three-point scheme is used, leading to a linear system of equations with a tri-diagonal matrix, unconditionally guaranteeing conservation and positivity preservation for positive state variables. For the advection part, total variation diminishing (TVD) schemes are used, which also ensure conservation and positivity preservation. For details, see Pietrzak (1998) and Leonard (1991).

Classical discretisations of the reaction terms, however, do not guarantee both—conservation (in the sense of Eq. 5) and non-negativity. The explicit schemes given by the Runge–Kutta hierarchy, the first-order forward Euler scheme E1 (Eq. 21), the second-order Runge–Kutta scheme RK2 (Eq. 22), and the fourth-order Runge–Kutta scheme RK4 (Eq. 23), are not unconditionally positivity preserving, see Burchard et al. (2003). The remedy for positivity preservation, the quasi-implicit Patankar-type schemes [motivated by the work of Patankar (1980), see also Deleersnijder et al. (1997)] are not conservative, since source and sink terms are numerically treated in a different way. For this type of schemes, the first-order Patankar–Euler scheme PE1 (Eq. 24), and the second-order Patankar–Runge–Kutta scheme PRK2 (Eq. 25), are considered here. In order to obtain conservative and unconditionally positivity preserving schemes, Burchard et al. (2003) suggested to treat both, sinks and sources quasi-implicitly, which leads to the first-order Modified Patankar–Euler scheme MPE1 (Eq. 26), and the second-order Modified Patankar–Runge–Kutta scheme MPRK2 (Eq. 27).

All these schemes will be tested here for their performance in a model problem with stiff reaction terms.

4 Numerical time scales and temporal accuracy of ODE solvers

4.1 Numerical time scales

Here, we will define time scales of the reaction part of the full problem (Eq. 1), which are numerically of high relevance. The ODE part of the biogeochemical model (Eq. 1) may be written as

$$d_t c_i = \sum_{j=1}^{I} p_{i,j}(\underline{c}) - \sum_{j=1}^{I} d_{i,j}(\underline{c}), \quad i = 1, \ldots, I. \tag{7}$$

For the first-order Euler forward scheme (see Eq. 21), the positivity preservation criterium is thus:

$$\frac{1}{\Delta t} > \frac{\sum_{j=1}^{I} d_{i,j}(\underline{c}^n) - \sum_{j=1}^{I} p_{i,j}(\underline{c}^n)}{c_i^n}, \tag{8}$$

which is guaranteed if

$$\Delta t < \frac{c_i^n}{\sum_{j=1}^{I} d_{i,j}(\underline{c}^n)} \quad \text{for all } i \text{ with } \sum_{j=1}^{I} d_{i,j} > 0. \tag{9}$$

For cases with $\sum_{j=1}^{I} d_{i,j} = 0$ no positivity violation will occur. It thus makes sense to define the numerical time scales

$$\tau_{i,j}^n = \frac{c_i^n}{d_{i,j}(\underline{c}^n)}, \tag{10}$$

giving the time scale of a destruction process from c_i to c_j. The positivity criterium (Eq. 9) is then formulated as

$$\Delta t \le \min_i \left(\sum_{j=1}^{I} \frac{1}{\tau_{i,j}^n} \right)^{-1} \Rightarrow \Delta t \le \min_{i,j} \tau_{i,j}^n. \tag{11}$$

The latter part of Eq. 11 gives a necessary (but not sufficient) condition for positivity preservation.

4.2 Temporal accuracy

In the temporal domain $0 \le t < \infty$, we consider the following ordinary differential problem:

$$d_t c = -\frac{c}{T}, \quad c(0) = c^0, \tag{12}$$

where c^0 and T represent the initial value of the function $c(t)$ and the relevant time scale of decay, respectively. As is well known, the solution to this problem is

$$c(t) = c^0 \exp\left(-\frac{t}{T}\right). \tag{13}$$

It is convenient to introduce dimensionless variables as follows:

$$t' = \frac{t}{T}, \quad c' = \frac{c}{c^0}. \tag{14}$$

Dropping the primes, to simplify the notations, the differential problem above and its solution may be rewritten as

$$d_t c = -c, \quad c(0) = 1, \quad c(t) = \exp(-t). \tag{15}$$

Thus, the dimensionless time scale of decay is unity.

When applying the numerical schemes discussed in Sect. Vertical discretisation and ODE solvers to the simple model problem (Eq. 15), it can be easily seen that the first-order schemes PE1 and MPE1 (see Eqs. 24, 26) and also the second-order schemes PRK2 and MPRK2 (see Eqs. 25, 27) perform identically. Thus, only five out the seven schemes discussed in Sect. Vertical discretisation and ODE solvers will be analysed here.

All these schemes lead to a discrete equation of the form:

$$c^{n+1} = \mu c^n, \tag{16}$$

where μ is a constant. As required by Eq. 15, $c^0 = 1$, yielding the solution

$$c^n = \mu^n. \tag{17}$$

If

$$0 < \mu < 1, \tag{18}$$

then the discrete solution decreases monotonically; otherwise, the discrete solution exhibits other types of behaviour. In other words, for the discrete solution to behave qualitatively as the exact one—which decreases monotonically—conditions (Eq. 18) are to be met. If Eq. 18 holds true, Eq. 17 may be rewritten as

$$c^n = \exp\left(-\frac{n\Delta t}{\tau}\right) \tag{19}$$

where the numerical time scale of decay is defined as

$$\tau = -\frac{\Delta t}{\ln \mu}. \tag{20}$$

Of course, the better the numerical scheme, the closer the corresponding time scale is to unity. For the numerical schemes mentioned above, the conditions (Eq. 18) for exhibiting monotonous decrease, the time scale of decay τ and its asymptotic behaviour as $\Delta t \to 0$ are readily estimated, see Table 1 and Fig. 1. It can be seen that the fully explicit schemes E1, RK2 and RK4 are monotonously decreasing only for $\Delta t/T < 1$, $\Delta t/T < 2$ and $\Delta t/T < 2.785$, respectively. The two positivity-preserving schemes have the same asymptotic behaviour for

Table 1 Numerical rate of decrease μ, stability range and asymptotic numerical time scale for the five different ODE solvers (Eqs. 21, 22, 23, 24, 25) applied to the exponential decay law (Eq. 15) discussed in Sect. Vertical discretisation and ODE solvers

	E1	RK2	RK4	PE1	PRK2
μ	$1-\Delta t$	$1-\Delta t+\frac{\Delta t^2}{2}$	$1-\Delta t+\frac{\Delta t^2}{2}-\frac{\Delta t^3}{6}+\frac{\Delta t^4}{24}$	$\frac{1}{1+\Delta t}$	$\frac{2}{2+2\Delta t+\Delta t^2}$
$0 < \mu < 1$	$0 < \Delta t < 1$	$0 < \Delta t < 2$	$0 < \Delta t < \Delta t^*$	$0 < \Delta t < \infty$	$0 < \Delta t < \infty$
τ as $\Delta t \to 0$	$\approx 1-\frac{\Delta t}{2}$	$\approx 1+\frac{\Delta t^2}{6}$	$\approx 1+\frac{\Delta t^4}{120}$	$\approx 1+\frac{\Delta t}{2}$	$\approx 1+\frac{\Delta t^2}{6}$

For Δt^* it is obtained $\Delta t^* = \frac{4}{3} - \frac{10}{3}\left(\frac{2}{43+9\sqrt{29}}\right)^{1/3} + \frac{2^{2/3}}{3}\left(43+9\sqrt{29}\right)^{1/3} \approx 2.785$. Note that scheme MPRK2 behaves asPRK2 and MPE1 behaves as PE1 for this simple underlying test problem

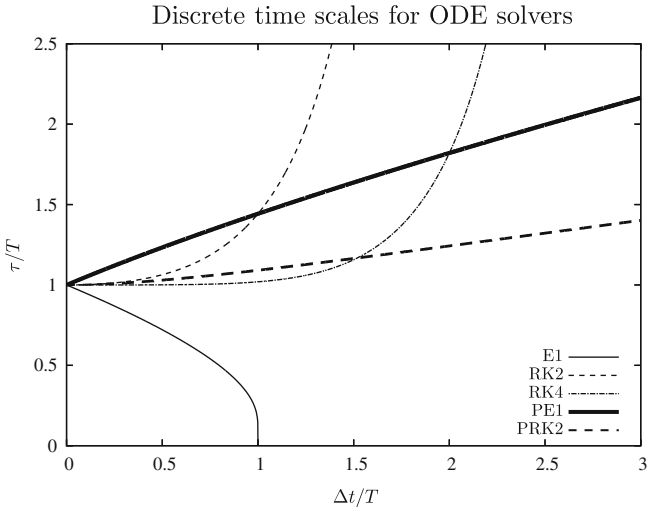

Fig. 1 Non-dimensional numerical time scales for the linear decay law according to Eq. 20 for the five different ODE solvers investigated in Sect. Temporal accuracy, see also Table 1

small time steps (with the opposite sign for E1 and PE1), but for larger time steps, their growth is close to linear. In contrast to that, the numerical time scales of the fully explicit schemes show growth towards infinity for finite time steps.

5 NPZD model

NPZD models have been developed for basic studies of the marine ecosystem, such as for better understanding the carbon cycle (see Oschlies and Kähler 2004; Popova et al. 2000). Their advantage is their low complexity with only four state variables and typically seven processes and consequently a fairly small number of adjustable empirical parameters. The processes reproduced by NPZD models are nutrient uptake by phytoplankton, grazing of herbivorous zooplankton on phytoplankton, mortality and excretion of phytoplankton and zooplankton, and remineralisation of dead or-

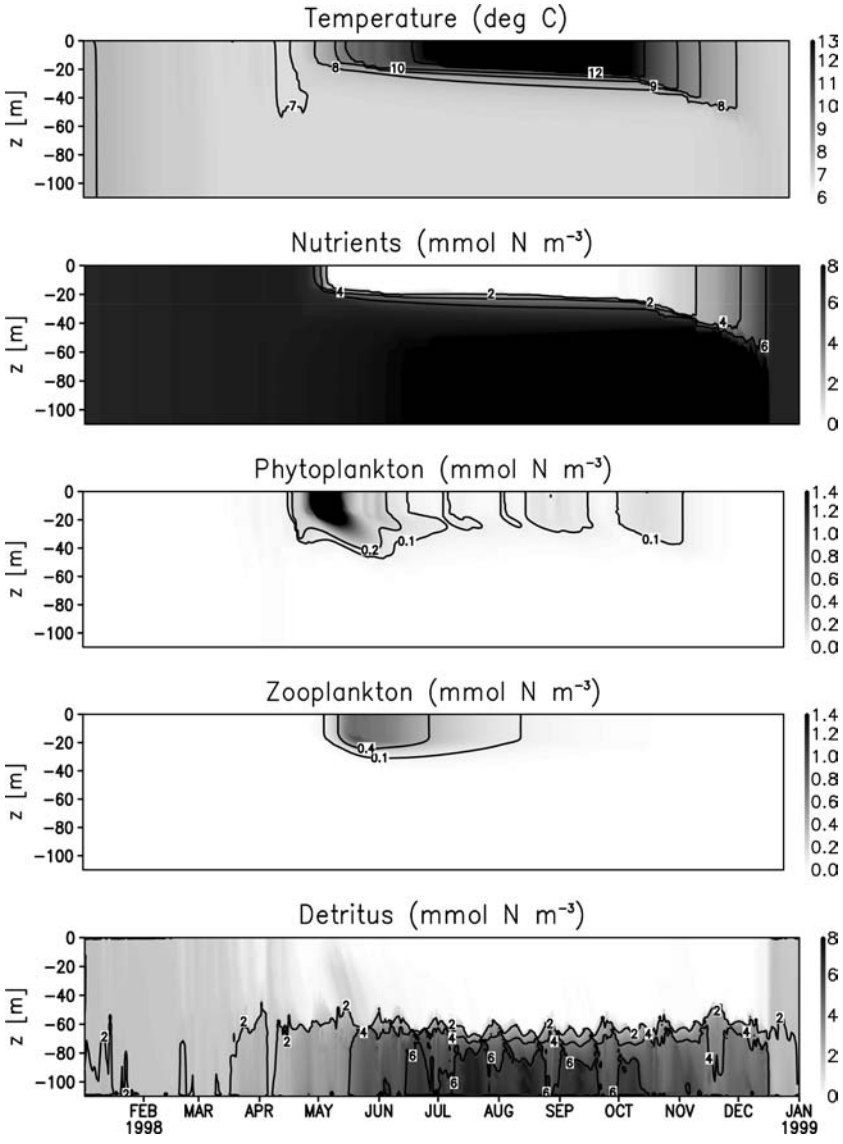

Fig. 2 Physical and biogeochemical model results for the application of the NPZD model to the Northern North Sea

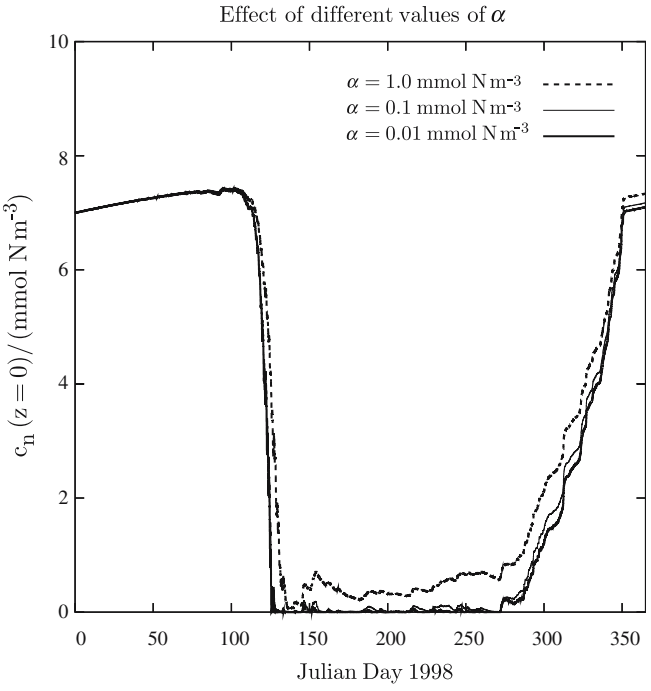

Fig. 3 Surface nutrient concentration for different values of α calculated at high temporal resolution with the MPE1 scheme

ganic matter into nutrients. Nutrient uptake (phytoplankton growth) is limited by light and nutrient availability, the latter of which is modelled by means of Michaelis–Menten kinetics, see Eq. 28. The half-saturation nutrient concentration α used in this formulation has typically a value between 0.2 and 1.5 mmol N m^{-3}, but in order to obtain a simple idealised stiff model problem for test purposes, we reduce α to values of 0.01 and 0.1 mmol N m^{-3} here. This has the consequence that nutrient is taken up by phytoplankton even at low concentrations, which strongly decreases the time scale of this process. The overall phytoplankton evolution over an annual cycle (as shown in Fig. 2) is not much affected by this manipulation, except from the fact that now the summer surface nutrient concentrations are much lower, see Fig. 3. It should be noted that such low half-saturation concentrations for nutrients have actually been observed in the oceanic mixed layer. Harrison et al. (1996) calculated for the mixed layer of the North Atlantic mean half saturation concentrations for nitrate and ammonium as small as 0.02 mmol N m^{-3}.

Zooplankton grazing which is limited by the phytoplankton standing stock is modelled by means of an Ivlev formulation, see Eq. 30. All other processes are based on linear first-order kinematics, see Eqs. 31, 32, 33, 34, 35. The surface and bottom fluxes of biogeochemical concentrations are set to zero, such that the total nitrogen content should be conserved, see also Fig. 7.

For all details of the NPZD model used here, see appendix NPZD model details.

6 Model simulations

6.1 Setup of model experiment

In order to provide a typical and clearly defined physical environment for testing the modified NPZD model discussed in Sect. NPZD model, we use an annual simulation of the water column in the Northern North Sea. The setup is similar to the one described and validated in detail by Bolding et al. (2002). The location was at 59°20′N and 1°E, at a mean water depth of about 110 m. For forcing this annual simulation, time series of surface slopes were extrapolated from observations obtained in autumn 1998 during the PROVESS project based on four partial tides by means of harmonic analysis. All necessary meteorological data are from the UK Meteorological Office Model. For calculating the resulting surface fluxes, the bulk formulae from Kondo (1975) are used. Deviating from Bolding et al. (2002), the absorption of incoming short-wave radiation has been computed by means of a bimodal function with attenuation lengths fitted to the Northern North Sea, see Kühn and Radach (1997). The photosynthetically available radiation (PAR) has been simply taken as 50% of the short-wave radiation, a feedback of increased turbidity due to plankton blooms to the light absorption has not been considered for the heat budget. For further details of the physical model setup, see Bolding et al. (2002).

All simulations carried out for the present study have been obtained with a time step of 2 h for the physical part. For the biogeochemical part, a time splitting has been introduced such that fractional time steps were possible for this part of the computation. Thus, by using a time step of $\Delta^{phy}t = 7{,}200$ s for the physical part and iterating the biogeochemical part 1, 4 and 36 times per physical time step with unchanged physical forcing, biogeochemical time steps of $\Delta^{bio}t = 7{,}200$ s, $\Delta^{bio}t = 1{,}800$ s and $\Delta^{bio}t = 200$ s, respectively, could be obtained. By doing so, it would be possible to use exactly the same physical forcing for all ODE solvers and all biogeochemical time steps, see also Burchard et al. (2004).

6.2 Model results

Many details of the physical model results have been shown by Bolding et al. (2002). In Fig. 2 we show the temperature evolution over the year 1998 as the only physical result. During winter and early spring, the water column is fully homogenised. From May onwards, a thermal stratification due to net heat transport into the water column develops, with peak temperatures in mid August of up to 15°C, and full erosion of the stratification in late November. During summer, the bottom mixed layer due to tidal activity and the surface mixed layer due to surface stress are separated by a thermocline, characterised by a low vertical exchange of mass, heat and momentum. Salinity gradients (not shown

here) play a minor, stabilising role. Phytoplankton shows a distinct bloom starting in late April, followed by a zooplankton peak feeding on the phytoplankton, see Fig. 2. Growth-limiting nutrients are depleted during summer, and only some erosion of the thermocline, which brings some nutrients into the euphotic zone, results in smaller intermediate phytoplankton peaks. Detritus (dead organic matter) which is fully mixed in winter, cannot pass the thermocline from below and thus stays in the bottom mixed layer during summer. The increased settling of detritus during mid May due to phytoplankton mortality is clearly visible in Fig. 2.

The results of the ecosystem model are here only given for clarity. The model has neither been calibrated for this specific situation, nor have the model results been validated against observational data. Apart from the half-saturation concentrations for nutrients, on which the overall evolution of the state variables does not strongly depend, all empirical model parameters are set to standard values.

In Fig. 4, the four numerically relevant time scales for phytoplankton as defined in Eq. 10 are shown for a high temporal resolution ($\Delta t = 20$ s) simulation with the RK4 scheme. Depending on the value chosen for the half saturation nutrient concentration, α, the time scale for nutrient uptake goes down to 2,442 s (for $\alpha = 0.1$ mmol N m^{-3}) and 201 s (for $\alpha = 0.01$ mmol N m^{-3}). In the latter case, the nutrient uptake time scale covers six orders of magnitude, such that this model problem may be regarded as stiff. The other three numerical time scales of the phytoplankton equation (for grazing, excretion and mortality) are larger than 10^6 s.

Model results for near surface nutrient concentration obtained with different ODE solvers and time steps are shown in Fig. 5. All results are compared to a reference solution obtained by means of a high-order scheme (RK4) with a short time step of $\Delta t = 20$ s. The explicit schemes E1 and RK4 both fail for time steps of 2 h and half an hour, since they predict strongly negative nutrient concentrations during summer. This is expected because of their conditional stability shown in Table 1 and Fig. 1. The positivity-preserving schemes PE1, PRK2, MPE1 and MPRK2 seem to perform well, since at the scale shown in Fig. 5 they are hardly distinguishable from the high-resolution reference solution. However, the two non-conservative schemes PE1 and PRK2 show significant deviations from the reference solution at the end of the simulation.

A closer look into the results during the first instance of nutrient depletion at day 125 reveals that both positivity-preserving first-order schemes (PE1 and MPE1) deviate substantially from the reference solution, whereas the positivity-preserving second-order schemes (PRK2 and MPRK2) are much closer to the reference solution, see Fig. 6. Specifically, the numerical solutions with time steps of half an hour are nearly indistinguishable from the reference solution even at this scale. This is remarkable, since the numerical time scale for the nutrient uptake is down to 201 s here, see Fig. 4. At this

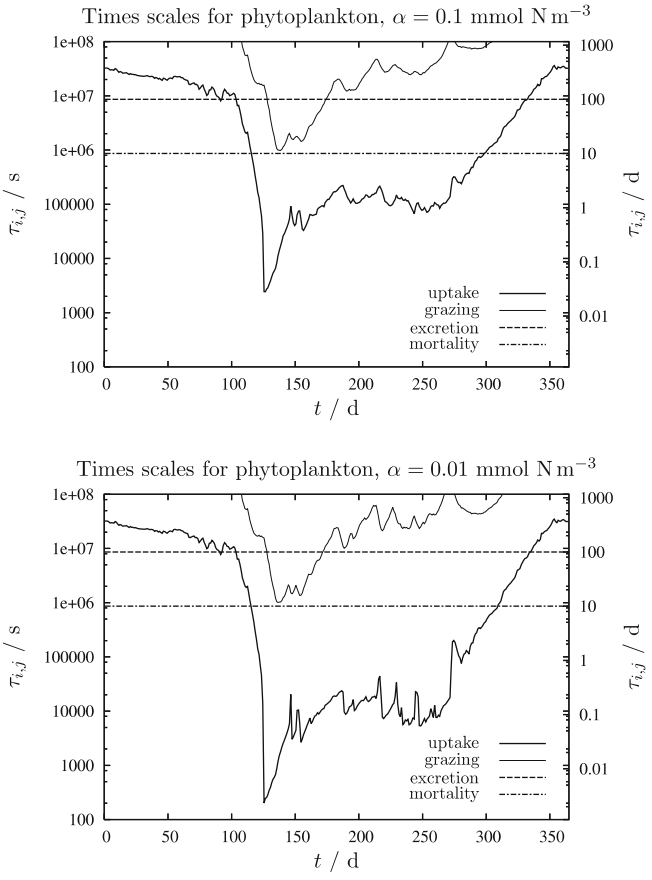

Fig. 4 Timescales for the phytoplankton equation in the NPZD model as defined in Eq. 10 during a one-year simulation. *Upper panel*: half saturation nutrient concentration $\alpha = 0.1$ mmol N m^{-3}; *lower panel*: $\Delta = 0.01$ mmol N m^{-3}. Shown are daily minimum values. *Bold*: nutrient uptake; *thin*: zooplankton grazing; *dashed*: phytoplankton excretion; *dash-dotted*: phytoplankton mortality. The fastest time scale in the upper panel is 2,442 s (approximately 41 min), the fastest time scale in the lower panel is 201 s (approximately 3 min)

point, the non-conservativity of the PRK2 scheme has seemingly no negative impact on the numerical solution.

Figure 7, however, shows how the total nitrogen conservation is significantly violated with the two non-conservative schemes PE1 and PRK2. The increase in total nutrient content is about 10% for the PE1 scheme at a time step of 2 h, and still about 0.7 % for the PRK2 scheme with a time step of half an hour. In contrast to that, the explicit schemes E1, RK2 and RK4 and the Modified Patankar-type schemes MPE1 and MPRK2 are conservative up to machine accuracy.

7 Conclusions

The stable, accurate and conservative performance of the second-order Modified Patankar–Runge–Kutta scheme (MPRK2), which has been developed by Burchard et al. (2003), has been demonstrated here for a stiff biogeochemical test problem for the water column.

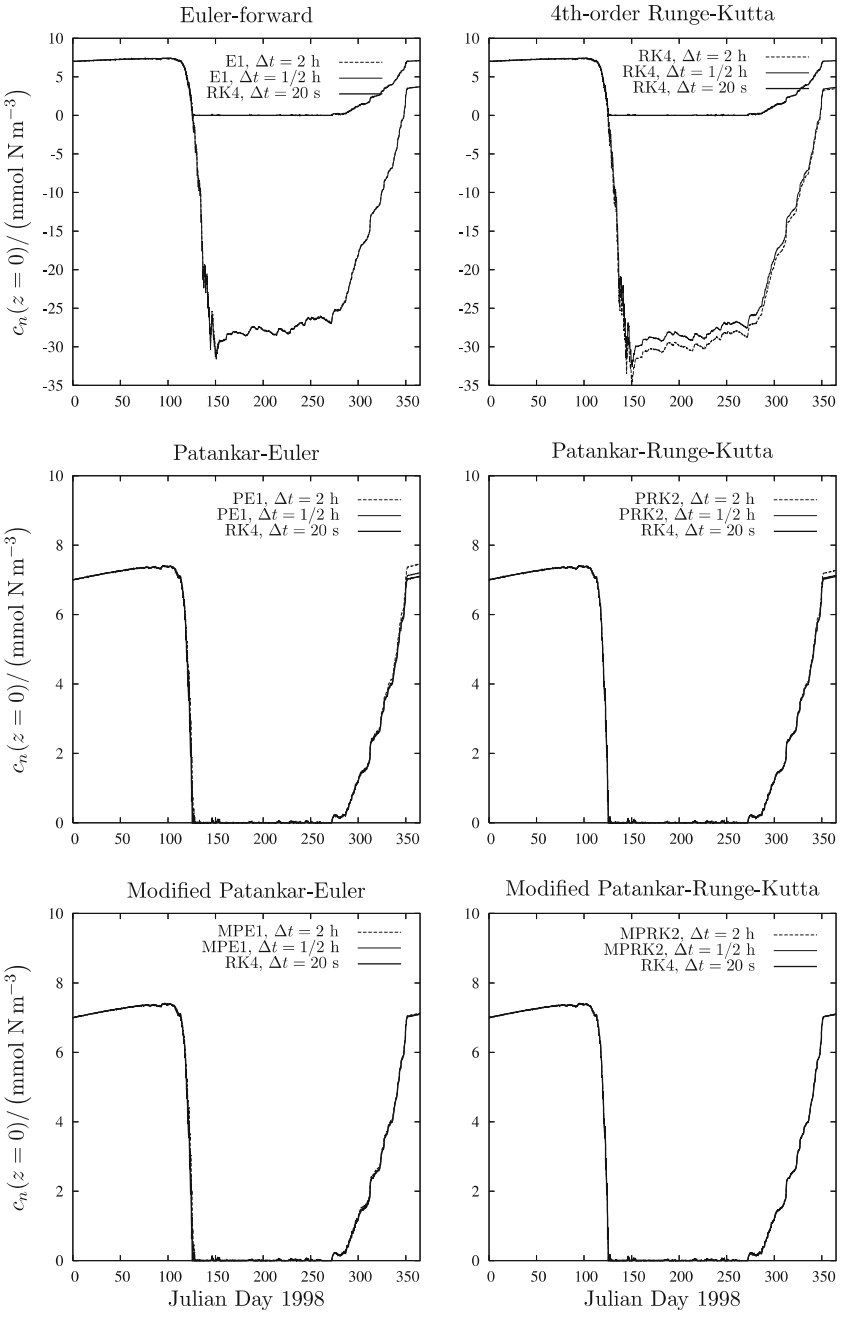

Fig. 5 Surface nutrient concentration for the simulation with $\alpha = 0.01$ mmol N m^{-3}. Six different ODE solvers with time steps of $\Delta t = 2$ h and $\Delta t = 1/2$ h are compared to the solution for the fourth-order Runge–Kutta scheme with $\Delta t = 20$ s. Note the different scales for the *upper two panels*

Also the first-order Modified Patankar–Euler scheme (MPE1) computed stable and conservative numerical results, but at a significantly smaller accuracy. All fully explicit schemes, the first-order Euler scheme (E1), the second-order Runge–Kutta scheme (RK2) and the fourth-order Runge–Kutta scheme (RK4) failed unless time steps smaller than the numerical time scale defined here were used. The non-conservative first-order Patankar–Euler scheme (PE1) and the second-order Patankar–Runge–Kutta scheme (PK2) computed results structurally similar to their Modified counterparts MPE1 and MPRK2, but the results showed a considerable conservation error.

Of course, also the numerical costs of the Modified Patankar schemes have to be taken into account. They are compared for all seven ODE solvers applied in the calculations here in Table 2. It is shown that for the first-order Modified Patankar–Euler scheme (MPE1) the run time is 1.5 times the run time of the model applying the first-order Euler scheme (E1) and the second-order Patankar–Runge–Kutta scheme (MPRK2) is 2.4 times the run time of the model applying the first-order Euler scheme (E1). Expressed in CPU times for the ODE solvers only, the second-order schemes need twice the run time as the corresponding first-order schemes, and the RK4 scheme

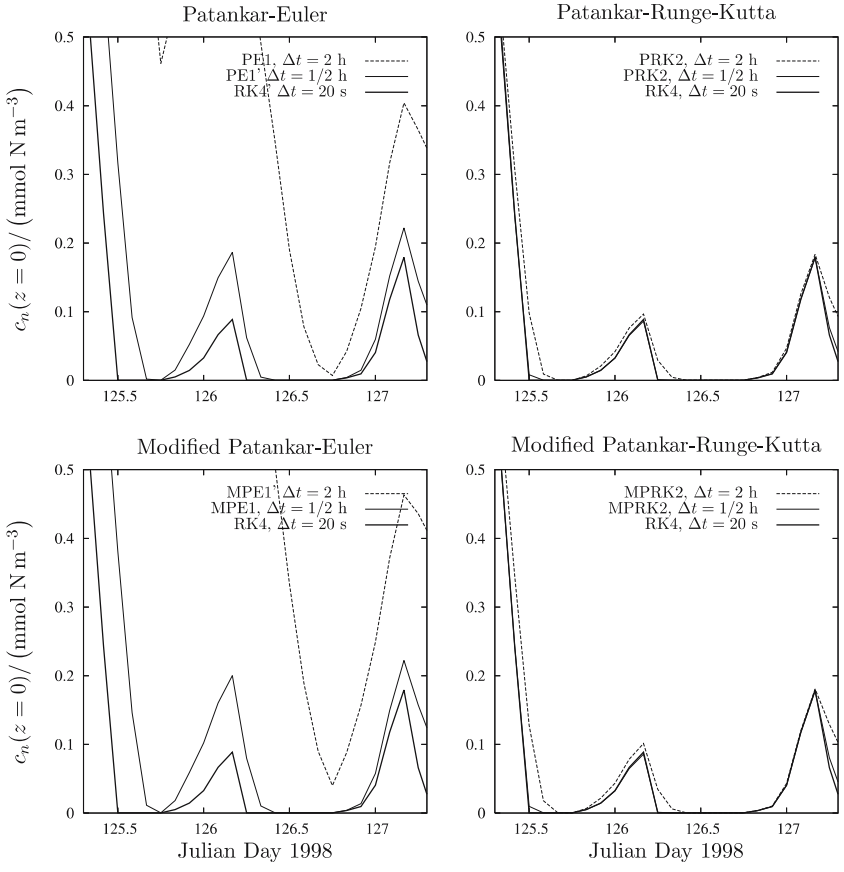

Fig. 6 Same as Fig. 5, but for a two-day period during the beginning of the nutrient depletion for the four positivity-preserving schemes described in appendix Discrete schemes for reaction terms

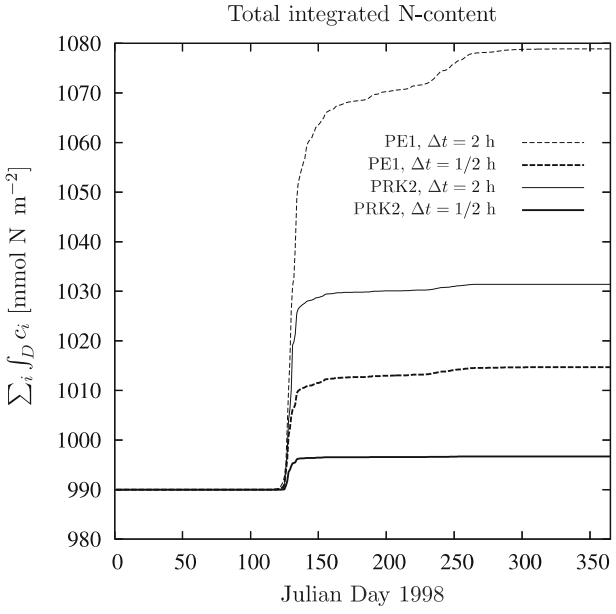

Fig. 7 Total content of nitrogen integrated over the water column obtained for the non-conservative first-order Patankar–Euler (PE1) and second-order Patankar–Runge–Kutta (PRK2) schemes for time steps of $\Delta t = 2$ h and $\Delta t = 1/2$ h

Table 2 Run time comparison

	E1	RK2	RK4	PE1	PRK2	MPE1	MPRK2
Total	1.0	1.4	2.0	1.1	1.5	1.5	2.4
ODE	1.0	2.0	4.0	1.3	2.5	2.4	4.7
ODE (%)	36	53	70	43	59	58	71

First two lines: factors by which model runs with more complex ODE solvers than the first-order Euler scheme (E1) use more CPU time; total: relative run time for the complete numerical part of the model; ODE: relative run time for the ordinary differential equation solver. The third line (ODE%) shows the ratio of the ODE solver run time to the total numerical run time in per cent for each scheme. These relative run times are rounded numbers and have been obtained by averaging over three model runs for each solver in order to filter out the small run time differences obtained by the compiler for identical model runs

needs 4 times the run time of the E1 scheme, which is clear since the right-hand sides are evaluated twice and 4 times, respectively, per each time step and vertical grid box. The Modified Patankar schemes are nearly double as expensive as the Patankar schemes and by a factor of nearly 2.5 more expensive than the explicit schemes E1 and RK2, respectively. This is in accordance with the findings of Burchard et al. (2003) who found 3 times longer run times for the MPRK2 scheme with respect to the E1 scheme for a non-linear ODE problem. The relatively long run times needed for the Modified Patankar schemes may be reduced by using faster solvers for linear systems than the classical Gaussian elimination. However, when taking into ac-

Table 3 State variables of the NPZD model

Variable	Meaning	Dimension
$c_1 = c_n$	Nutrient	mmol N m^{-3}
$c_2 = c_p$	Phytoplankton	mmol N m^{-3}
$c_3 = c_z$	Zooplankton	mmol N m^{-3}
$c_4 = c_d$	Detritus	mmol N m^{-3}

count that the time step for the E1 scheme would have to be reduced from 7,200 s to 200 s (a factor of 36) in order guarantee positive near-surface nutrient concentrations (see Figs. 4, 5), the factors of 1.5 or 2.4 for the total run times required by the MPE1 and the MPRK2 schemes with respect to the E1 scheme schemes, respectively, are not that significant.

Although most biogeochemical models are not as stiff as the model problem investigated here, they also may result in negative concentrations at larger time steps, see e.g. Burchard et al. (2005) with simulations of the Fasham et al. (1990) model. Thus, the use of the MPRK2 scheme is recommended also for model problems with sink and source terms which are not obviously stiff.

As further testing of the Modified Patankar schemes, applications to chemical advection-diffusion reaction problems with typically stiff reaction terms would be needed. Such problems occur, for example, in marine sediments and in the iron cycle of the water column. For problems without transport terms, Burchard et al. (2003) have already shown the stable, accurate and conservative behaviour for the stiff Robertson test problem (see Robertson 1966).

Acknowledgements Substantial parts of this work were carried out during a visit of Hans Burchard in Louvain-la-Neuve, funded by the Institut d' Astronomie et de Géophysique G. Lemaître of the Université Catholique de Louvain. Eric Deleersnijder is a Research Associate with the Belgian National Fund for Scientific Research (FNRS) and his contribution to the present study was made in the scope of the project "A second-generation model of the ocean system", which is funded by the Communauté Française de Belgique (Actions de Recherche Concertée) (see http://www.astr.ucl.ac.be/SLIM). We are grateful to Karsten Bolding (Baaring, Denmark) who has provided the computational framework for the biogeochemical calculations carried out here. Finally, we acknowledge the critical comments of two anonymous reviewers who helped us to substantially improve the manuscript.

Appendix

8 Discrete schemes for reaction terms

In this section, the ODE solvers used in the present investigation are given. Here, $\underline{c}^n = (c_i^n)_{i=1,\ldots,I}$ represents the discrete result vector at the old time step and $\underline{c}^{n+1} = (c_i^{n+1})_{i=1,\ldots,I}$ at the new time step.

8.1 Conservative schemes

First-order Euler-forward (E1)

$$c_i^{n+1} = c_i^n + \Delta t\{P_i(\underline{c}^n) - D_i(\underline{c}^n)\}. \tag{21}$$

Second-order Runge–Kutta (RK2)

$$\left.\begin{aligned} c_i^{(1)} &= c_i^n + \Delta t\{P_i(\underline{c}^n) - D_i(\underline{c}^n)\}, \\ c_i^{n+1} &= c_i^n + \tfrac{\Delta t}{2}\left\{P_i(\underline{c}^n) + P_i\left(\underline{c}^{(1)}\right) - D_i(\underline{c}^n) - D_i\left(\underline{c}^{(1)}\right)\right\}. \end{aligned}\right\} \tag{22}$$

Fourth-order Runge–Kutta (RK4)

$$\left.\begin{aligned} c_i^{(1)} &= c_i^n + \Delta t\{P_i(\underline{c}^n) - D_i(\underline{c}^n)\}_i^{(2)} \\ &= c_i^n + \Delta t\left\{P_i\left(\tfrac{1}{2}\left(\underline{c}^n + \underline{c}^{(1)}\right)\right) - D_i\left(\tfrac{1}{2}\left(\underline{c}^n + \underline{c}^{(1)}\right)\right)\right\}_i^{(3)} \\ &= c_i^n + \Delta t\left\{P_i\left(\tfrac{1}{2}\left(\underline{c}^n + \underline{c}^{(2)}\right)\right) - D_i\left(\tfrac{1}{2}\left(\underline{c}^n + \underline{c}^{(2)}\right)\right)\right\}_i^{(4)} \\ &= c_i^n + \Delta t\left\{P_i\left(\underline{c}^{(3)}\right) - D_i\left(\underline{c}^{(3)}\right)\right\}_i^{n+1} \\ &= \tfrac{1}{6}\left\{c_i^{(1)} + 2c_i^{(2)} + 2c_i^{(3)} + c_i^{(4)}\right\}. \end{aligned}\right\} \tag{23}$$

8.2 Positivity-preserving schemes

First-order Patankar–Euler scheme (PE1)

$$c_i^{n+1} = c_i^n + \Delta t\left\{P_i(\underline{c}^n) - D_i(\underline{c}^n)\frac{c_i^{n+1}}{c_i^n}\right\}. \tag{24}$$

Second-order Patankar–Runge–Kutta (PRK2)

$$\left.\begin{aligned} c_i^{(1)} &= c_i^n + \Delta t\left\{P_i(\underline{c}^n) - D_i(\underline{c}^n)\frac{c_i^{(1)}}{c_i^n}\right\}, \\ c_i^{n+1} &= c_i^n + \tfrac{\Delta t}{2}\left\{P_i(\underline{c}^n) + P_i\left(\underline{c}^{(1)}\right) - \left(D_i(\underline{c}^n) + D_i\left(\underline{c}^{(1)}\right)\right)\frac{c_i^{n+1}}{c_i^{(1)}}\right\}. \end{aligned}\right\} \tag{25}$$

8.3 Conservative and positivity-preserving schemes

First-order modified Patankar–Euler scheme (MPE1)

$$c_i^{n+1} = c_i^n + \Delta t\left\{\sum_{j=1}^{I} p_{i,j}(\underline{c}^n)\frac{c_j^{n+1}}{c_j^n} - \sum_{j=1}^{I} d_{i,j}(\underline{c}^n)\frac{c_i^{n+1}}{c_i^n}\right\}. \tag{26}$$

Second-order modified Patankar–Runge–Kutta (MPRK2)

$$\left.\begin{aligned} c_i^{(1)} &= c_i^n + \Delta t \left\{ \sum_{j=1}^{I} p_{i,j}(\underline{c}^n) \frac{c_j^{(1)}}{c_j^n} - \sum_{j=1}^{I} d_{i,j}(\underline{c}^n) \frac{c_i^{(1)}}{c_i^n} \right\}, \quad i^{n+1} \\ &= c_i^n + \frac{\Delta t}{2} \left\{ \sum_{j=1}^{I} \left(p_{i,j}(\underline{c}^n) + p_{i,j}\left(\underline{c}^{(1)}\right) \right) \frac{c_j^{n+1}}{c_j^{(1)}} - \sum_{j=1}^{I} \left(d_{i,j}(\underline{c}^n) + d_{i,j}\left(\underline{c}^{(1)}\right) \right) \frac{c_i^{n+1}}{c_i^{(1)}} \right\}. \end{aligned}\right\} \tag{27}$$

9 NPZD model details

The NPZD model described in Sect. NPZD model consists of $I=4$ state variables, see Table 3.

Seven processes expressed as sink terms are included in this conservative model, see Eqs. 28, 29, 30, 31, 32, 33, 34, 35.

Nutrient uptake by phytoplankton

$$d_{np} = r_{\max} \frac{I_{\mathrm{PAR}}}{I_{\mathrm{opt}}} \exp\left(1 - \frac{I_{\mathrm{PAR}}}{I_{\mathrm{opt}}}\right) \frac{c_n}{\alpha + c_n} c_p \tag{28}$$

Table 4 Empirical constants used for the NPZD model

Parameter	Meaning	Value	References
α	Half saturation	0.01...0.1 mmol N m^{-3}	[28]
$r_{\max}$	Maximum uptake rate	1.0 day^{-1}	[28]
$g_{\max}$	Maximum grazing rate	0.5 day^{-1}	[30]
$I_{\min}$	Minimum PAR	25 W m^{-2}	[28]
I_v	Ivlev constant	1.1 (mmol N m^{-3})$^{-1}$	[30]
r_{dn}	$D \rightarrow N$ rate (remineralisation)	0.003 day^{-1}	[33]
r_{pd}	$P \rightarrow D$ rate (P mortality)	0.02...0.1 day^{-1}	[34]
r_{pn}	$P \rightarrow N$ rate (P excretion)	0.01 day^{-1}	[31]
r_{zd}	$Z \rightarrow D$ rate (Z mortality)	0.02 day^{-1}	[35]
r_{zn}	$Z \rightarrow N$ rate (Z excretion)	0.01 day^{-1}	[32]
w_d	Settling velocity for detritus	-5 m day^{-1}	[1]
w_p	Settling velocity for phytoplankton	-1 m day^{-1}	[1]

Most of the values have been adopted from Fennel and Neumann (1996). The mortality of phytoplankton, r_{pd} depends on the light availability, it is set to $r_{pd}=0.02$ day^{-1} in the euphotic zone ($I_{\mathrm{PAR}} \geq I_{\min}$) and to $r_{pd}=0.1$ day^{-1} below the euphotic zone ($I_{\mathrm{PAR}} < I_{\min}$). Deviating from standard literature, the half saturation constant for nutrients, α, is here set to two different low values in order to obtain a stiff model problem

with

$$I_{\mathrm{opt}} = \max\left(\frac{1}{4} I_{\mathrm{PAR}}, I_{\min}\right). \tag{29}$$

Grazing of zooplankton on phytoplankton

$$d_{pz} = g_{\max}\left(1 - \exp\left(-I_v^2 c_p^2\right)\right) c_z \tag{30}$$

Phytoplankton excretion

$$d_{pn} = r_{pn} c_p \tag{31}$$

Zooplankton excretion

$$d_{zn} = r_{zn} c_z \tag{32}$$

Remineralisation of detritus into nutrients

$$d_{dn} = r_{dn} c_d \tag{33}$$

Phytoplankton mortality

$$d_{pd} = r_{pd} c_p \tag{34}$$

Zooplankton mortality

$$d_{zd} = r_{zd} c_z \tag{35}$$

All empirical parameters for the NPZD model are given in Table 4.

References

Abdulle A (2001) Fourth order Chebyshev methods with recurrence relations. SIAM J Sci Comp 23:2042–2055

Abdulle A, Medovikov AA (2001) Second order Chebyshev methods based on orthogonal polynomials. Numer Math 90:1–18

Bolding K, Burchard H, Pohlmann T, Stips A (2002) Turbulent mixing in the Northern North Sea: a numerical model study. Cont Shelf Res 22:2707–2724

Burchard H, Deleersnijder E, Meister A (2003) A high-order conservative Patankar-type discretisation for stiff systems of production-destruction equations. Appl Numer Math 47:1–30

Burchard H, Bolding K, Kühn W, Meister A, Neumann T,Umlauf L (2005) Description of a flexible and extendable physical-biogeochemical model system for the water column. J Mar Sys (in press)

Deleersnijder E, Beckers J-M, Campin J-M, El Mohajir M, Fichefet T, Luyten P (1997) Some mathematical problems associated with the development and use of marine models. In: Diaz JI (ed) The mathematics of models for climatology and environment, vol 48. of NATO ASI Series, Springer, Berlin Heidelberg New York, pp 41–86

Fasham MJR, Ducklow HW, McKelvie SM (1990) A nitrogen-based model of plankton dynamics in the oceanic mixed layer. J Mar Res 48:591–639

Fennel W, Neumann T (1996) The mesoscale variability of nutrients and plankton as seen in a coupled model. Dt Hydrogr Z 48:49–71

Hairer E, Wanner G (2004) Solving ordinary differential equations II, Series in computational mathematics 14, 3rd edn. Springer, Berlin Heidelberg New York

Hairer E, Nørsett S, Wanner G (2000) Solving ordinary differential equations I, Series in computational mathematics 8, 2nd edn. Springer, Berlin Heidelberg New York

Harrison WG, Harris L, Irwin BD (1996) The kinetics of nitrogen utilization in the oceanic mixed layer: nitrate and ammonium interactions at nanomolar concentrations. Limnol Oceanogr 41:16–32

Horváth Z (1998) Positivity of Runge–Kutta and diagonally split Runge–Kutta methods. Appl Numer Math 28:309–326

van der Houwen PJ (1996) The development of Runge–Kutta methods for parabolic differential equations. Appl Num Math 20:261–273

van der Houwen PJ, Sommeijer BP (1980) On the internal stability of explicit m-stage Runge–Kutta methods for large m-values. ZAMM 60:479–485

Hundsdorfer W, Verwer JG (2003) Numerical solution of time-dependent advection-diffusion-reaction equations0, vol 33 of Series in computational mathematics. Springer, Berlin Heidelberg New York

Kondo J (1975) Air-sea bulk transfer coefficients in diabatic conditions. Bound Layer Meteor 9:91–112

Kühn W, Radach G (1997) A one-dimensional physical-biological model study of the pelagic nitrogen cycling during the spring bloom in the northern North Sea (FLEX'76). J Mar Res 55:687–734

Lebedev V (2000) Explicit difference schemes for solving stiff problems with a complex or separable spectrum. Comp Math Math Phys 40:1729–1740

Leonard BP (1991) The ULTIMATE conservative difference scheme applied to unsteady one-dimensional advection. Comput Meth Appl Mech Eng 88:17–74

Medovikov AA (1998) High order explicit methods for stiff ordinary differential equations. BIT 38:372–390

Meister A (1998) Comparison of different Krylov subspace methods embedded in an implicit finite volume scheme for the computation of viscous and inviscid flow fields on unstructured grids. J Comput Phys 140:311–345

Oschlies A, Kähler P (2004) Biotic contribution to air-sea fluxes of CO_2 and O_2 and its relation to new production, export production, and net community production. Global Biogeochemical Cycles 18. GB1015, doi:10.1029/2003GB002094

Patankar SV (1980) Numerical heat transfer and fluid flow. McGraw-Hill, New York

Pietrzak J (1998) The use of TVD limiters for forward-in-time upstream-biased advection schemes in ocean modeling. Mon Weather Rev 126:812–830

Popova EE, Ryabchenko VA, Fasham MJR (2000) Biological pump and vertical mixing in the southern ocean: their impact on atmospheric CO_2. Global Biogeochem Cycles 14:477–498

Robertson HH (1966) The solution of a set of reaction rate equations. In: Walsh J (ed) Numerical analysis, an introduction. Academic, New York, pp 178–182

Sandu A, Verwer J, van Loon M, Carmichael G, Potra F, Dabdub D, Seinfeld J (1997) Benchmarking stiff ODE solvers for atmospheric chemistry problems I: Implicit versus explicit. Atmos Environ 31:3151–3166

Soetaert K, Herman PMJ, Middelburg JJ (1996) A model of early diagenetic processes from the shelf to abyssal depths. Geochim Cosmochim Acta 60:1019–1040

Verwer JG (1996) Explicit Runge–Kutta methods for parabolic partial differential equations. Appl Num Math 22:359–379

Weber L, Völker C, Schartau M, Wolf-Gladrow DA (2005) Modelling the speciation and biochemistry of iron at the Bermuda Atlantik Time-series Study site, Global Biogeochemical Cycles, 19. doi:10.1029/2004GB002340